This published paper can be found in: Integrated Ferroelectrics,
Volume 58, Issue 1 2003, pg 1347-1357

A MODEL OF PHASE TRANSITION KINETICS IN LEAD SCANDIUM TANTALATE THIN FILMS

J. BATTAT, Z. HUANG, [a]P.P. DONOHUE,
AND R.W. WHATMORE
Department of Advanced Materials, SIMS, Cranfield University,
Beds MK43 0AL, UK;
[a]QinetiQ, St. Andrews Rd., Malvern, Worcs WR14 3PS, UK

The phase transformations from amorphous to pyrochlore to perovskite in lead scandium tantalate (PST) thin films during rapid thermal annealing process (RTA) have been studied by X-ray diffraction (XRD) techniques. The growth and decay of the pyrochlore phase, the growth of the perosvkite PST were analysed using the Avrami model. Integral equations have been derived and numerical calculation been used to simulate the volume fractions for pyrochlore and perovskite as functions of annealing time. Transformation parameters k and n were obtained by comparing the simulated to the experimental intensities using a least-squares curve fitting technique. Activation energies for perovskite formation were calculated. The results indicate that the phase transitions are diffusion-limited. TEM, SEM, and EDS were employed to study the lead loss and other factors affecting phase transitions.

Keywords: Lead Scandium Tantalate (PST); phase transition; kinetics; thin film

INTRODUCTION

Lead Scandium Tantalate (PST) is a very promising material in uncooled infrared (IR) radiation sensors for a wide range of applications such as fire alarms, intruder detection and thermal imaging because of its high figure of merit for IR detection [1-2]. Recent effort has been focused on the growth of PST as thin films directly onto silicon wafers in order to lower cost and improve device performance [3].

The formation of perovskite PST can generally be divided into two categories: in-situ growth of perovskite PST, or deposition of PST into a non-perovskite form followed by a post-deposition anneal step to achieve perovskite conversion. For monolithic IR detectors the thermal budget for PST deposition is limited by the underlying CMOS circuitry which suffers from thermally induced degradation of the Al-Si interconnect metallization [3]. Recently there has been a move away from the fully monolithic approach for PST based detectors in order to remove these thermal budget limitations and enable high merit figures for IR detection to be realized [4]. In this composite thermal detectors the arrays of microbridges are fabricated on an interconnect wafer, able to withstand temperatures of up to 1000 °C, which is then flip-chip bonded to the ROIC [4].

It has been shown that the use of excess lead during the sputtering deposition promotes the formation of perovskite PST [5-6]. Todd et. Al [6-7] reported growth of perovskite PST at 530 °C by using sputtering techniques. However, in-situ perovskite PST sputtering at elevated temperature can lead to difficulties with lead compositional control and problems with equipment reliability. Therefore a low temperature deposition followed by a separate post-deposition anneal was preferred. They also showed that PST deposited at 450 °C formed a very well crystallised pyrochlore phase which was difficult to completely transform to perovskite during post-deposition annealing. A deposition temperature of 300 °C resulted in a weak pyrochlore/amorphous phase that could be completely transformed to perovskite by a post-deposition rapid thermal anneal (RTA), although not within the CMOS thermal budget. The processing regime was however well within the thermal budget of the interconnect wafer [4]. Conventional oven annealing was also tried but the slow heat-up rates resulted in incomplete conversion to perovskite, due to lead loss from the PST film by diffusion and evaporation, and consequently inferior electrical properties compared to RTA annealed films [8].

Extensive research has been reported on the ordering of PST, however, only limited reports have been devoted to the crystallisation and very little if any on the kinetics of phase transitions of perovskite PST from its amorphous or pyrochlore phases. In this paper we report our study on the kinetics of phase transitions from amorphous to pyrochlore then to perovskite in PST thin films.

EXPERIMENTAL

The substrates used were (100)-Si single crystal wafers which were thermally oxidised and overcoated with a sputtered platinum/titanium(Pt/Ti) layer. The PST was deposited by sputtering in a custom sputtering system which uses dual 8" diameter RF magnetron sputtering targets in an argon/10% oxygen atmosphere. More details have been published elsewhere [6-7]. The as-deposited wafer was cut into several pieces of squares about 10 mm x 10 mm, and each piece was then subjected to a series of RTA and structural characterisation processes.

The Avrami equation [9-10] has been widely used to model the kinetics of phase transitions. The equation is:

$V(t) = 1 - \exp(- k t^n)$,

where V(t) is the transformed fraction at time t, n is the Avrami coefficient whose value normally varies from 1 to 3 [10] and k a rate constant. Mathcad 7 (MathSoft®) software was used to simulate intensity profiles as functions of annealing time.

RESULTS AND DISCUSSION

Theoretical Consideration

It is well established that upon annealing PST undergoes transitions from amorphous (A) to pyrochlore (Py) then to perovskite (Pe), which can be represented as follows:

$$x \xrightarrow{k_1,n_1} y \xrightarrow{k_2,n_2} z$$

here x, y, and z are the volume fractions of the amorphous, pyrochlore and perovskite phases respectively, n_1,k_1,n_2, and k_2 are transformation parameters in Avrami equation. Therefore

$$x+y+z=1 \quad \ldots\ldots\ldots\ldots\ldots\ldots..(1)$$

From Avrami equation the amorphous phase fraction x at time t is:

$$x = \exp(-k_1 t^{n_1}) \quad \ldots\ldots\ldots\ldots\ldots\ldots..(2)$$

therefore $\frac{dx}{dt} = k_1 n_1 t^{n_1 - 1} x$ ………………(3)

If there is an amount r of the pyrochlore phase which for some reasons does not transform into perovskite, then the pyrochlore y can be divided into two parts: an active component y_a, which undergoes the transformation into z and is therefore dependent on all four transformation parameters n_1,k_1,n_2, and k_2, and a component y_r which only undergoes transformation from the amorphous but does not convert into z, and therefore is only dependent on parameters n_1 and k_1. i.e.,

$$y = y_a + y_r$$

we do not know the exact time profile of the y_r, but it is plausible to assume that the formation of this part of the pyrochlore also follows Avrami equation, i.e.,

$$y_r = r \cdot \left(1 - e^{-k_1 t^{n1}}\right), \qquad \ldots\ldots\ldots\ldots\ldots(4)$$

therefore

$$\frac{dy_r}{dt} = rn_1 k_1 t^{n_1 - 1} e^{-k_1 t^{n1}} \qquad \ldots\ldots\ldots\ldots\ldots\ldots..(5)$$

According to the Avrami equation, at any time t we also have

$$\frac{dz}{dt} = k_2 n_2 t^{n_2 - 1} y_a \qquad \ldots\ldots\ldots\ldots\ldots\ldots\ldots(6)$$

combining the above equations gives

$$\frac{dy_a}{dt} = \frac{-dx}{dt} - \frac{dz}{dt} - \frac{dy_p}{dt} = (1-r)n_1 k_1 t^{n_1 - 1} e^{-k_1 t^{n1}} - k_2 n_2 t^{n_2 - 1} y_a \qquad \ldots\ldots\ldots\ldots\ldots..(7)$$

which is a first order differential equation and can be manipulated to give the following

solution for $y = y_r + y_a = r \cdot \left(1 - e^{-k_1 t^{n1}}\right) + y_a$: :

$$y(t) = r \cdot \left(1 - e^{-k_1 t^{n1}}\right) + (1 - r) \cdot e^{-k_2 t^{n}} \cdot \int_0^t n_1 k_1 \tau^{n_1 - 1} \cdot e^{-k_1 \tau^{n1}} \cdot e^{k_2 \tau^{n2}} d\tau \qquad \ldots\ldots\ldots\ldots\ldots\ldots\ldots\ldots..(8)$$

Substitutes the expression for y_a to equation (6) gives the following expression for z:

$$z(t) = (1 - r) \cdot \int_0^t k_2 n_2 \tau^{n_2 - 1} e^{-k_2 \tau^{n2}} \cdot \left[\int_0^\tau n_1 k_1 \theta^{n_1 - 1} e^{-k_1 \theta^{n1}} e^{k_2 \theta^{n2}} d\theta\right] d\tau \qquad \ldots\ldots\ldots\ldots\ldots\ldots\ldots(9)$$

Let y(t) and z(t) represents the theoretical volume fractions of the pyrochlore and perovskite phases at time t respectively, py and pe the corresponding experimental values. Parameters n_1, k_1, n_2, and k_2 can be obtained by minimise the sum of the squares of the errors (SSE) which was defined as:

$$SSE(n_1, k_1, n_2, k_2) = \sum_i (py_i - Y(t_i))^2 + (pe_i - Z(t_i))^2 \qquad \ldots\ldots\ldots\ldots\ldots(10)$$

with summarisation over all the experimental points for the film RTA'ed at a particular temperature.

Transformation Parameters Determination

FIGURE 1 shows XRD patterns for a film PST700 after RTA'ed at 700 °C for 5,110, and 2000 seconds, the intensity scale being logarithmic and the spectra for 110 and 2000 s being vertically displaced to aide interpretation. Initially, there was a very strong presents of pyrochlore, as indicated by the strong peaks of pyrochlore (Py) (222) and (400); perovskite (Pe) (222) appeared after 5 s of RTA, Pe(200) and Pe(220) peaks were observable after 10 to 15 seconds. A broad hump around 2θ = 19, indicating the ordering Pe(111), started to appear after 290 s. After 2000 s, the Py(400) was still apparent and it had a normalised intensity 0.13. This pyrochlore did not decrease upon further annealing at this temperature therefore considered as the non-convertible pyrochlore y_r.

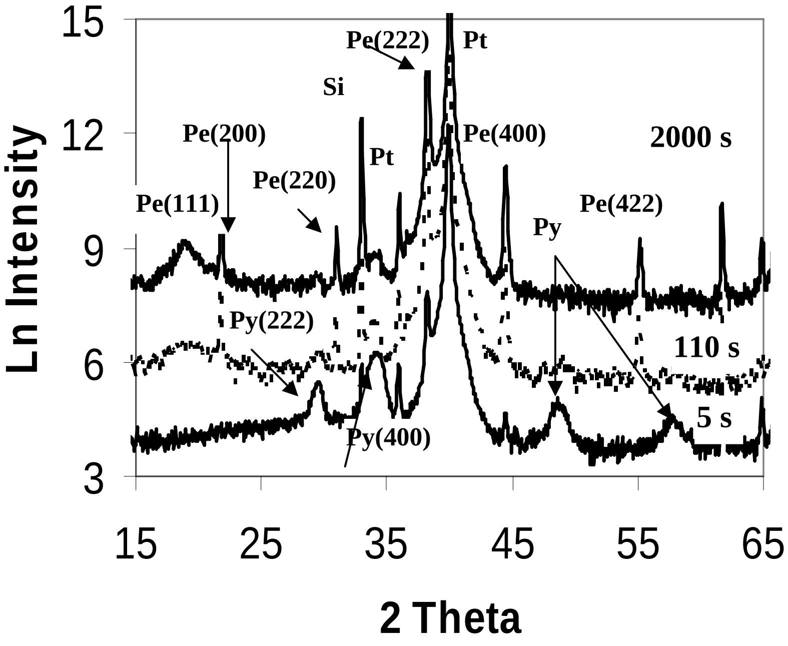

FIGURE 1: XRD patterns of PST thin films after rapid thermal annealing at 700 ˚C for 5, 110 and 2000 s respectively.

The volume fractions of the Py and Pe phase (marked by x and ◊ respectively) as functions of annealed time as plotted in FIGURE 2b, theoretical curves of y(t) and z(t) (solid line and dotted-line respectively), as obtained by finding the best fitting parameters n_1, k_1, n_2, and k_2, are also shown in FIGURE. 2b. FIGURE 2a, c and d show the simulated curves y(t) and z(t) as compared with the respective experimental data for

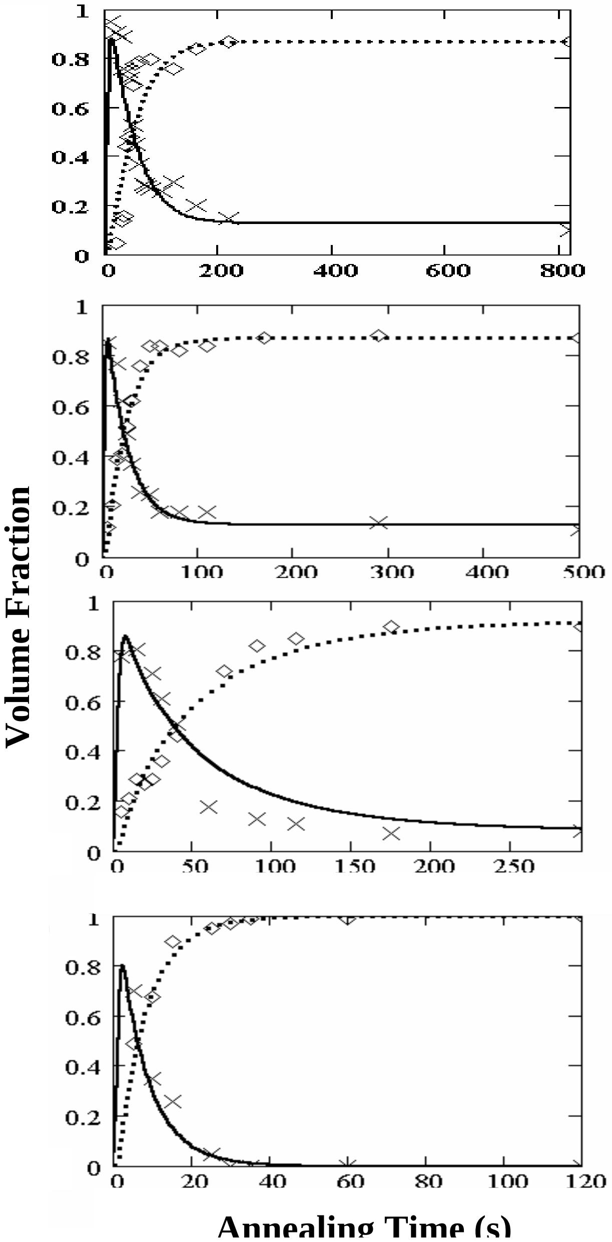

FIGURE 2 Experimental volume fractions (x and ◊ for pyrochlore and perovskite respectively) as functions of annealed time (seconds) as compared to the simulated (solid and dotted lines for the pyrochlore and perovskite respectively) curves for the PST thin films annealed at temperatures (a) 650 °C; (b) 700 °C; (c) 725 °C; and (d) 750 °C .

temperatures 650, 725 and 750 °C respectively. It can be seen that there is a good agreement between the simulated and the experimental values. The best-fitting parameters for all the temperatures are summarised in Table 1. It can be seen that n_l was close to 2 and n_2 close to 1. The amount of residue pyrochlore r which could not be converted into perovskite are listed in the last column of the table.

Table 1: Summary of phase transformation parameters.

Temperature (˚C)	n_l	k_l	n_2	k_2	r
650	2.13	0.02	1.22	0.0078	0.13
700	2.06	0.09	1.04	0.038	0.13
725	1.65	0.12	0.8	0.049	0.08
750	2.02	0.53	0.96	0.15	0

Arrhenius plots of rate constant k_2 against the inverse of temperature (1/T) for the transition from the pyrochlore to perovskite is shown in FIGURE 3. The trend line equation (Ln k ~ 1/Tx1000 x) is $K_2 = -26.4x_2 + 23.8$, from which the transformation activation energy could be determined as being 219 KJ/mol.

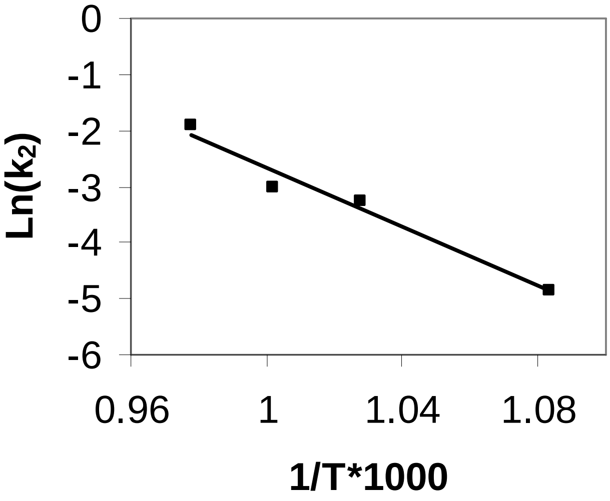

FIGURE 3 Arrhenius plots of rate constant ln k against the inverse of temperature (1/Tx1000) for the transition from the pyrochlore to perovskite PST.

The Avrami coefficients n_l as obtained from the model for the transformation from amorphous to pyrochlore, were very close to 2 for three temperatures 650, 700 and 750 ˚C and not largely deviated from 2 for the temperature 725 ˚C. This suggests a diffusion controlled pyrochlore growth, with decreasing nucleation rate [10]. This is in good agreement with observations in PZT system where a high-number density of small pyrochlore grains appeared initially upon annealing from the amorphous matrix, the number-density of the pyrochlore grains decreased in the latter stages of the annealing when perovskite phase was formed [11]. The Avrami coefficients n_2 as obtained for the transformation from pyrochlore to perovskite were very close to 1 for three temperatures 650, 700 and 750 ˚C and not largely deviated from 1-1.5 for the temperature 725 ˚C, suggesting also a diffusion controlled growth, without further nucleation after the initial stage [10]. This is also similar to the PZT system where the Avrami coefficient for the perovskite formation was found close to unity [11].

Structural Characterisation

FIGURE 4a, b, c and d show cross section TEM micrographs the films RTA'ed at 650, 700, 725 and 750 ˚C respectively. Two kinds of morphologies were observed—one with sub-layered structure and another without. Films annealed at 650, 700 and 750 ˚C all showed columnar-like perovskite structure and sub-layers. A first thought might be that these sub-layers are related to the repeated RTA annealing. However, no link between the number of sub-layers and the repeated times of RTA annealing was observed, e.g. there were 21 sub-layers in the PST700 but there were only 15 times of repeated annealing. A close inspection found that the sub-layers were formed by the horizontal linear distribution of voids. Vertical linear distribution of voids can also be seen in the film PST650. There were no regular distribution of voids in the films PST725 therefore no showing of sub-layer-like features.

SEM investigation on the final annealed films revealed no significant difference in surface morphologies among the films annealed at different temperatures. Perovskite PST grains were up to 500 nm in diameter and all the films had cracks. No apparent second phase grains were observed. Results of the compositional analysis for the films are summarised in Table 2. It can be seen that there was about 10% excess lead for the as-deposited film and some lead was lost during RTA treatment. However, there was an insignificant compositional difference between the films annealed at different temperatures and overall the films were Pb-excess.

Table 2 : Summary of SEM EDX results, all results in atomic percent.

	O	Sc	Ta	Pb
PST as deposited	59.11	9.31	9.04	22.55
PST650	59.63	9.66	9.63	21.08
PST700	59.59	10.13	9.4	20.88
PST725	59.87	10.09	9.8	20.24
PST750	59.69	9.57	9.72	21.02
PST stoichiometry	60	10	10	20

CONCLUSIONS

PST thin films for pyroelectric application have been deposited by rf sputtering and transformed into the desired perovskite structure by rapid thermal annealing. The film structures were characterized by XRD, TEM, SEM and EDS and its phase transition kinetics was analysed by using Avrami equation. Integral equations have been derived and numerical calculation been used to simulate the volume fractions for pyrochlore and

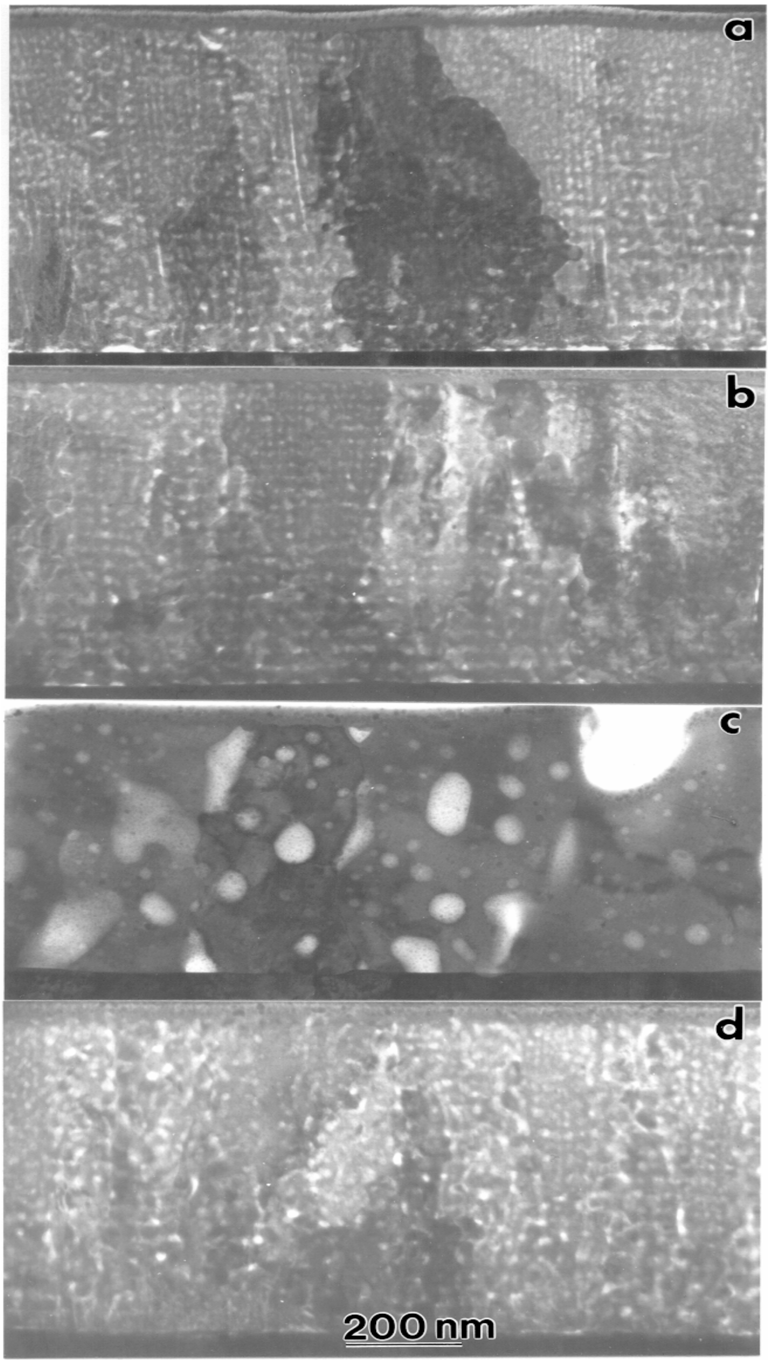

FIGURE 4 TEM cross section micrographs for PST thin films after RTA treatment at temperatures (a) 650; (b)700: (c)725 and (d) 750 °C.

perovskite as functions of annealing time. Transformation parameters k and n were obtained by comparing the simulated to the experimental intensites using a least-squares curve fitting technique. Activation energy for the perovskite formation calculated.

Acknowledgments

This work was financially supported by EPSRC platform grant, UK Ministry of Defence and TDK.

References

[1] R. W. Whatmore, Rep. Prog. Phys. **49** 1335 (1986).

[2] P. Muralt, Rep. Prog. Phys. **64** 1339 (2001).

[3] R. W. Whatmore and R. Watton, Pyroelectric materials and devices *Infrared Detectors and Emitters: Materials and Devices*, edited by P. Capper and C.T. Elliott, Kluwer Academic Publishers, London (2001).

[4] M. A. Todd, P. Manning, P. P. Donohue, A. G. Brown and R. Watton, SPIE **4130** 128 (2000).

[5] C. D. Meekison, K. Z. Baba-Kishi, R. Watton and M. A. Todd, Integrated Ferroelectrics **4** 25 (1994).

[6] M. A. Todd, P. P. Donohue, M. A. Harper and J. C. Jones, Integrated Ferroelectrics **35**, 115 (2001).

[7] M. A. Todd, P. P. Donohue, J. C. Jones, D. J. Wallis, M. J. Slater, M. A. Harper and R. Watton, Integrated Ferroelectrics **25** 113 (1999).

[8] Z. Huang, P. P. Donohue, M. A. Todd, J. C. Jones and R. W. Whatmore, J. Phys. D: Appl. Phys. **34** 3121 (2001).

[9] M. Avrami, J. Chem. Phys., **7**, 1103 (1939); **8**, 212 (1940); **9**, 177 (1941).

[10] J. Christian, "The Theory of Phase Transformation in Metals and Alloys", 2nd ed., Pergmon Press, Oxford, pp534-542 (1975).

[11] Huang Z, Zhang Q and Whatmore R W 1999 *J. Appl. Phys.* **85,** 7355 and **86** 1662.

A model of phase transition kinetics in lead scandium tantalate thin films

Battat, J.

2003

Battat J, Huang Z, Donohue PP, Whatmore RW. (2003) A model of phase transition kinetics in lead scandium tantalate thin films. Integrated Ferroelectrics, Volume 58, Issue 1, pp. 1347-1357

http://hdl.handle.net/1826/1747